Analysis of Microstructure Changes for AlSi9Cu3 Alloy Caused by Remelting

Dana Bolibruchová, Marek Matejka
University of Zilina, Faculty of Mechanical Engineering, University of Zilina, Zilina. Slovak Republic. E-mail: danka.bolibruchova@fstroj.uniza.sk, marek.matejka@fstroj.uniza.sk

The use of recycled or remelted alloys is one of the most common ways to reduce production costs. As the number of remelting increases, also chance of the chemical composition and the microstructure alteration is increasing, which has a major impact on the resulting mechanical properties. The microstructure of recycled alloys mostly affects the presence of iron and its negative effect on casting properties. The paper deals with the degree and the way of influence of the remelting on the microstructure of AlSI9Cu3 alloy with increased iron content to 1.4 wt. %. In the work are progressively evaluated changes of microstructures focused on the morphology and shape of the iron phases, dendritic structure change and pore formation due to remelting on AlSI9Cu3 alloy after natural aging and after the heat treatment (T5). The obtained results point to degradation of the microstructure due to multiple remelting with the possibility of partial improvement when applying heat treatment (T5).

Keywords: AlSi alloy, Remelting, Metallography, Fe phase

1 Introduction

Recycled or multiple-remelting alloys are a common material used in foundries and their quality is a key factor in keeping the resulting casting standard. It is a returnable material from foundry (gating systems, risers, ingots, etc.), which is used as a batch material to reduce costs. An important question in using such a material is how many times the material has been remelted. The extent and way of influencing the casting properties is the main reason for examining the effect of multiple remelting. With the increasing number of remelting may occur structural changes, changes in chemical composition, as well as the influence of mechanical and casting properties [1-3].

Recycled aluminum alloys, compared to primary alloys, contain an increased amount of iron, which negatively affects most properties of aluminum alloys. Iron with other elements present in Al-Si-Fe-Cu alloys form intermetallic phases such as Al_3Fe, Al_7FeCu_2, Al_8Fe_2Si, Al_5FeSi. Phase Al_5FeSi, also known as β-phase, has a greater impact on structure and mechanical properties than α-phase. It has a plate shape and represent a needle-like shape when observed on microstructure. The presence of long planks of this phase supports the initiation of fatigue tears and increases porosity because it interferes with the flowing melt in the interdental areas during solidification [4-7].

With the increasing iron and chromium content due to remelting and the presence of manganese as an iron corrector, may lead to creating so called "sludge phases" in the alloy. They represent hard inclusions characterized by high density with a tendency to segregate at the bottom of the melt in the holding furnaces [8-9]. From the crystallographic aspect, they are AlFeMnSi polyendic phases formed by perithetic reaction, which are not created during crystallization, but they are already present in the molten metal while holding the melt at low temperature or at a rapid cooling rate of the melt. The presence of sludge phases in the alloy leads to degradation of the mechanical properties of alloys. The amount of these particles will depend, in particular, on the amount of iron, chromium, manganese, which can be formulated by the sludge factor:

$$\boldsymbol{SF} = [\%\,\boldsymbol{Fe}] + \mathbf{2}\,.\,[\%\,\boldsymbol{Mn}] + \mathbf{3}\,.\,[\%\,\boldsymbol{Cr}] \quad (1)$$

Gobrecht and Jorstad have constructed a straight line based on an empirical relationship that applies to Al-Si-Cu alloys. The relationship represent the dependence between the sludge factor and the minimum holding temperature below which the alloy tends to form sludge phases. The sludge phases cannot be remelted, therefore it is necessary for keeping the melt at a sufficiently high temperature [10-11].

2 Materials and experiments procedure

To analyze the effect of increased iron content at multiple remelting, the maximum amount of iron in the alloy determined by the standard (1.1 wt. %) was increased. The alloy was "polluted" with the master alloy AlFe10, resulting in iron content approximately of 1.4 wt. %. Secondary alloy with higher iron content was used in the next experimental procedure as the reference alloy marked D1. The chemical composition is shown in Tab. 1. Subsequently, the reference alloy was subjected to a 6-time remelting. Each remelting consisted of casting ingots into prepared metal molds. After solidification and cooling, these ingots were used as batch for further melting without additional components addition. Samples were cast from each of the second melt, with marks D3, D5, and D7. The temperature of the metal mold was set at 100 ± 5 ° C and the casting temperature was in the range of 750 to 770 ° C. Structural analysis was performed on samples after naturally aging (about 160 hours at 20 ° C) and on samples after heat treatment (T5 - artificially aging at 200 ± 5 °C for 4 hours and cooling in water) [12].

Tab. 1 *Chemical composition of the AlSi9Cu3 alloy after addition of Fe*

Elements (wt. %)	**Si**	**Fe**	**Cu**	**Mn**
	9.347	1.416	1.741	0.178
Elements (wt. %)	**Mg**	**Ti**	**Cr**	**Sr**
	0.427	0.034	0.025	<0.002

3 Results

3.1 Microstructure analysis

Naturally aging

The reference alloy microstructure (D1) after natural aging consists of the α-phase matrix, the eutectic silicon excluded in the called unmodified form and intermetallic iron base (β - phase) in the form of thin needles (Fig. 1a). The increase in the number of the remelting resulted in the rounding (spheronization) of eutectic silicon, which was observed in a modified form, i.e., in a circular or elongated shape. The change also occurred in the shortening of the iron phase in the whole volume (Fig. 1b). The next increase of the remelting did not significantly affected the shape of the eutectic silicon nor the morphology of the iron, but the increase in their dimensions can be observed (Fig. 1c). The alloy microstructure after the 7th remelting (Fig. 1d) is characterized by long thin needles of the iron-based phase and the slightly coarsed grains of eutectic silicon as compared to the alloys D3 and D5.

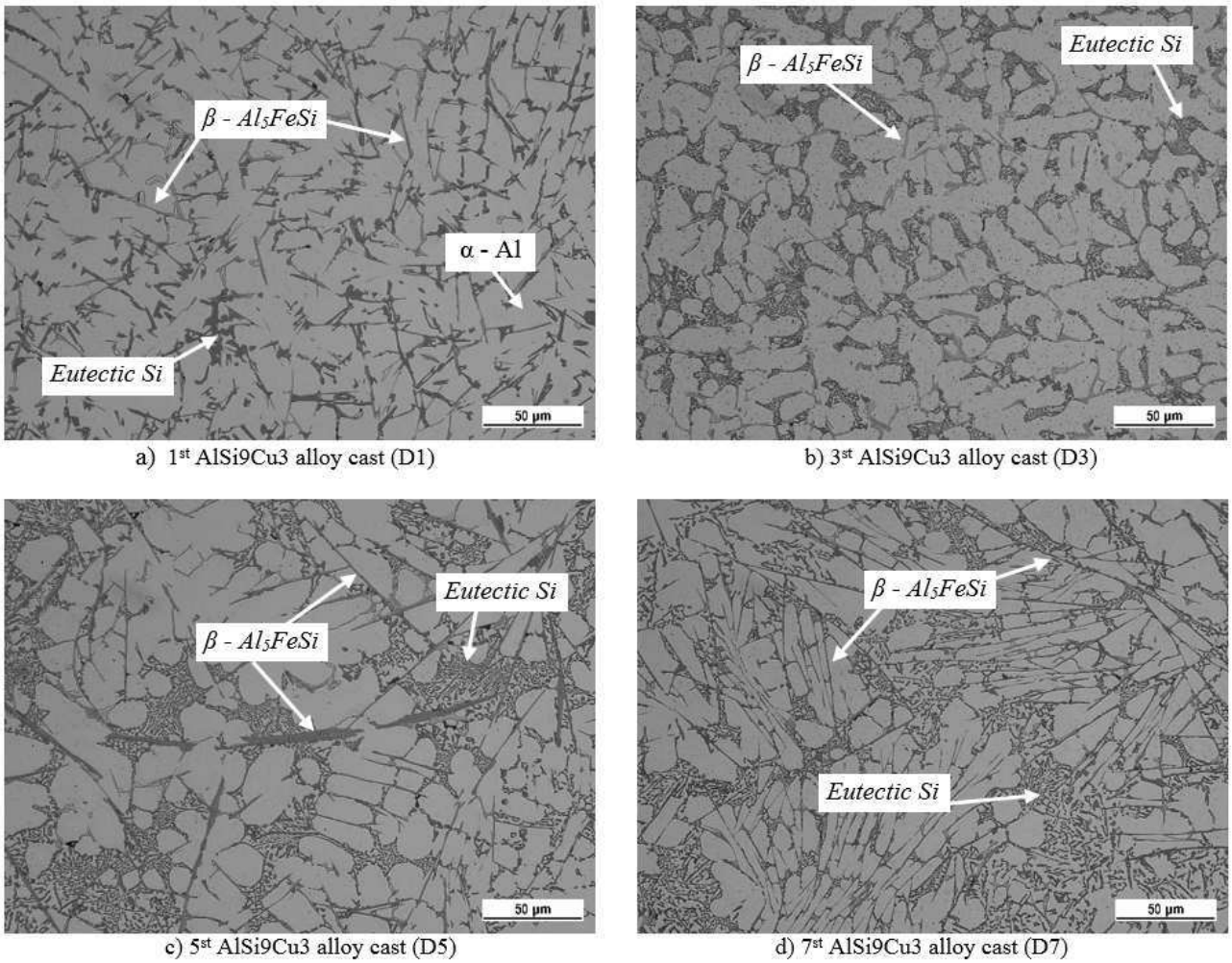

Fig. 1 *Optical micrographs showing microstructure of AlSi9Cu3 alloy after Naturally aged*

Heat treatment (T5 - artificially aging)

The effect of heat treatment on the alloy microstructure is documented in Fig. 2. It can be seen from the optical micrographs that the eutectic silicon at the reference alloy D1 (Fig. 2a) is present in an imperfect circular shape between the dimensional forms of β-Al5FeSi phase. For alloys D3 (Fig. 2b) and D5 (Fig.2c), eutectic silicon is in a modified form similar to that of alloys after naturally aging. In the alloy for the 7th remelting of D7 (Fig. 2d), there was no complete spheronization of eutectic silicon. Due to the heat treatment, the D3 and D5 alloys were locally refined in the iron-based phase.

For description of the remelting influence on the change of iron-based intermetallic phases in the form of needles was performed measurement of their lengths. Tab. 2 shows the average measured length of β-Al5FeSi phase for each alloy. The average length of the needle in the D1 alloy after natural aging reached 55.7 µm. After the addition of two additional melts, the length was reduced by about half to 27.7 µm. Subsequent remelting, a rapid increase in the length of iron-phase phases was observed in the structure of alloys D5 and D7 up to the maximum measured value of 89.4 µm. The effect of heat treatment was reflected in shortening the length of the needles in all alloys except the alloy D3, where approximately the same length of the iron-based intermetallic phase was measured. In fig. 3 is a graphical comparison of the change in the length of the needle after naturally aging and after heat treatment.

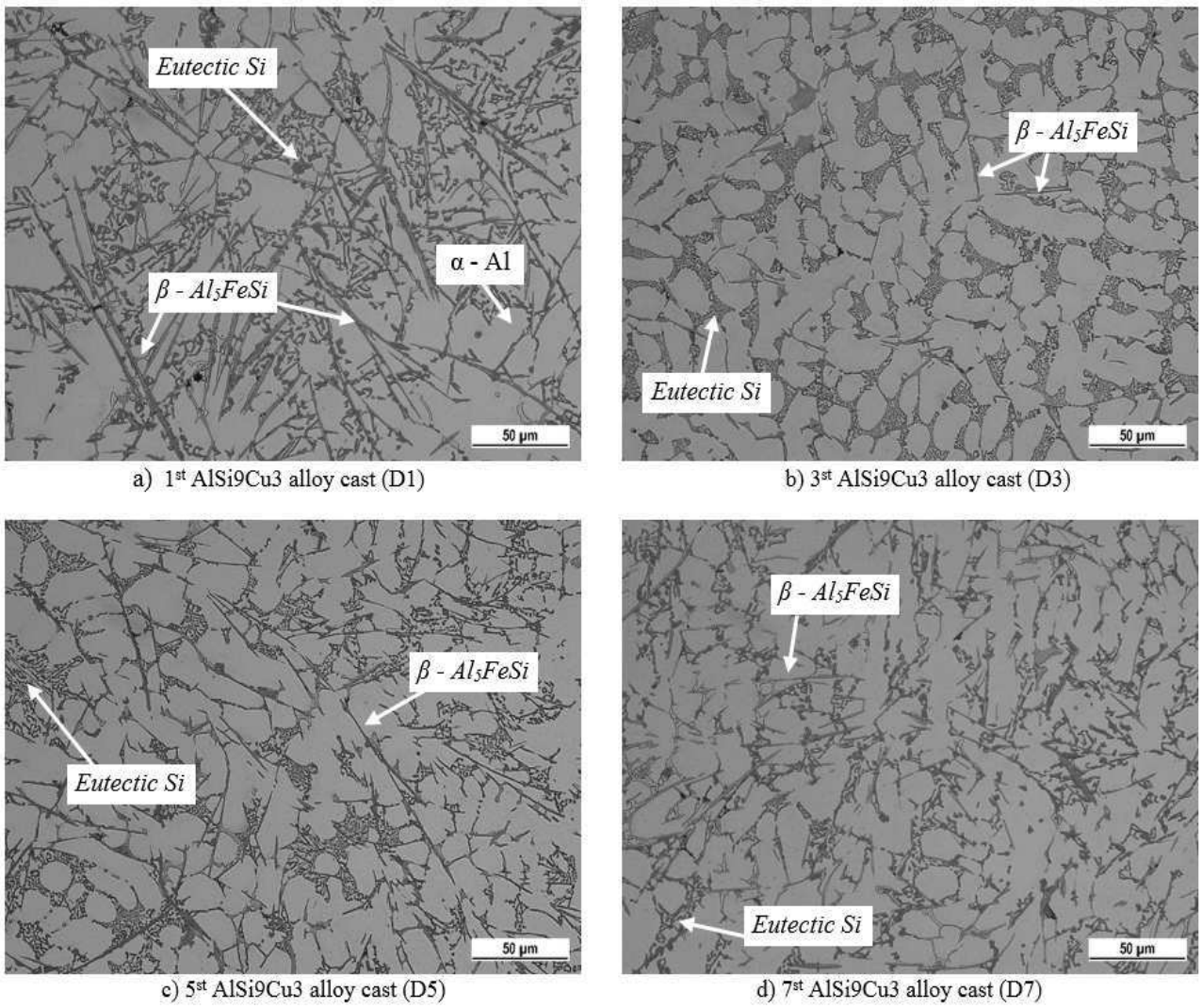

Fig. 2 *Optical micrographs showing microstructure of AlSi9Cu3 alloy after Artificially aged (T5)*

Tab. 2 *Results of measurements of length of iron based particles*

Cast number		D1	D3	D5	D7
Length of iron phases (µm)	Natural aged	55.7	27.7	71.4	89.4
	Artificial aged	37.8	26.3	55.1	72.6

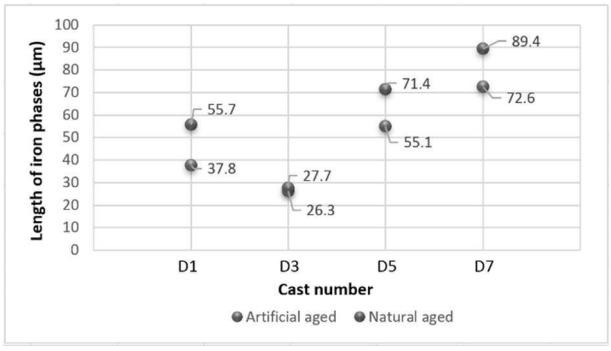

Fig. 2 *Relationship between Length of iron phases and cast number*

In tab. 3 are the changes in wt. % of selected elements depending on the amount of remelting. The chemical composition of the alloy is an important factor that influences the process of formation of intermetallic compounds. Depending on the chemical composition of the alloy, the harmful effect of iron occurs when the critical value of Fekrit in the wt. % is achieved:

$$Fe_{crit} \approx 0.075\, x\, (\%\, Si) - 0.05 \qquad (2)$$

The critical iron level for each melt was calculated according to equation (2). Exceeding the critical iron content in each alloy can be expected to produce a greater amount of intermetallic iron-based phases. At the same tab. 3 is also the ratio of manganese and iron for each melt. The Mn and Fe ratios are an important parameter in the prediction of iron phase segregation in a unfavourable needle form. Due to the lower ratio Mn / Fe in alloys than the recommended value (Mn / Fe ≥ 0.5), the increase in the probability of the iron phase of the needle morphology was increased. These assumptions were confirmed in microstructural analysis.

Tab. 3 *Relationship between wt. % Fe, Mn, Cr, Si, Fe_{crit} and ratio Mn/Fe and cast number (CN)*

CN	D1	D2	D3	D4	D5	D6	D7
Fe [wt. %]	0.178	0.176	0.186	0.221	0.181	0.196	0.187
Mn [wt. %]	1.416	1.475	1.51	1.705	1.738	1.809	1.889
Cr [wt. %]	0.025	0.027	0.04	0.046	0.065	0.093	0.106
Si [wt.%]	9.347	9.35	9.306	9.073	9.302	9.323	9.179
Fe_{crit} [wt. %]	0.651	0.651	0.648	0.63	0.647	0.649	0.638
Mn/Fe	0.16	0.12	0.12	0.13	0.1	0.11	0.09

The dendritic structure was evaluated by measuring the distance of the secondary axes of dendrites, referred to as the DAS factor. The measured DAS factor values for each alloy are shown in tab. 4. Despite the presence of a large number of iron-based intermetallic phases in the alloys, the values moved to a low level in the range of 17.1 µm to 20.2 µm. The preservation of the fine dendritic structure even in alloys with higher numbers of melting showed that the increasing number of remelting had no influence on the change in the dendritic structure of the alloys studied.

Tab. 4 *Results of measurements of DAS index*

Cast number		D1	D3	D5	D7
DAS (µm)	Natural aged	18.1	18.2	17.6	20.2
	Artificial aged	20.1	17.1	19.1	18.6

Using equation (1), the sludge factor was calculated for each alloy. The results of the sludge factor (SF), together with the minimum holding temperatures, depending on the number of remelting (CN), are shown in Tab. 5. Minimum holding temperatures for each remelt were obtained on the basis of the graph (Fig. 4) showing the relationship between the sludge factor and the minimum holding temperature below which the alloy has a tendency for the formation of the sludge phases. It can be seen in the graph that with the increasing number of melts, the holding temperature increases, thereby increasing the probability of the sludge phase formation in the melt at the same holding temperature. The presence of sludge phases is observed in the optical micrographs of the alloy D5 (Fig. 5a) and D7 (Fig. 5b), thus confirming the assumption of their occurrence in alloys with higher number of remelting.

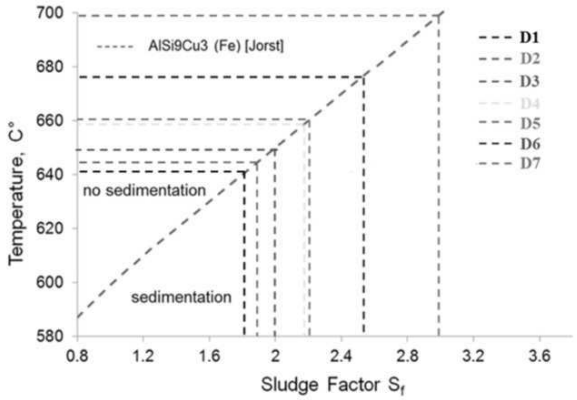

Fig. 4 *Values of minimum holding temperatures of alloys D1 to D7 derived from relationship between sludge factor and temperature*

Tab. 5 *Relationship between sludge factor (SF) and Values of minimum holding temperatures of alloys (T_{min}) and cast number (CN)*

CN	D1	D2	D3	D4	D5	D6	D7
SF	1.847	1.91	2.002	2.285	2.295	2.48	2.89
T_{min} [°C]	640 ± 5	645 ± 5	650 ± 5	659 ± 5	661 ± 5	675 ± 5	700 ± 5

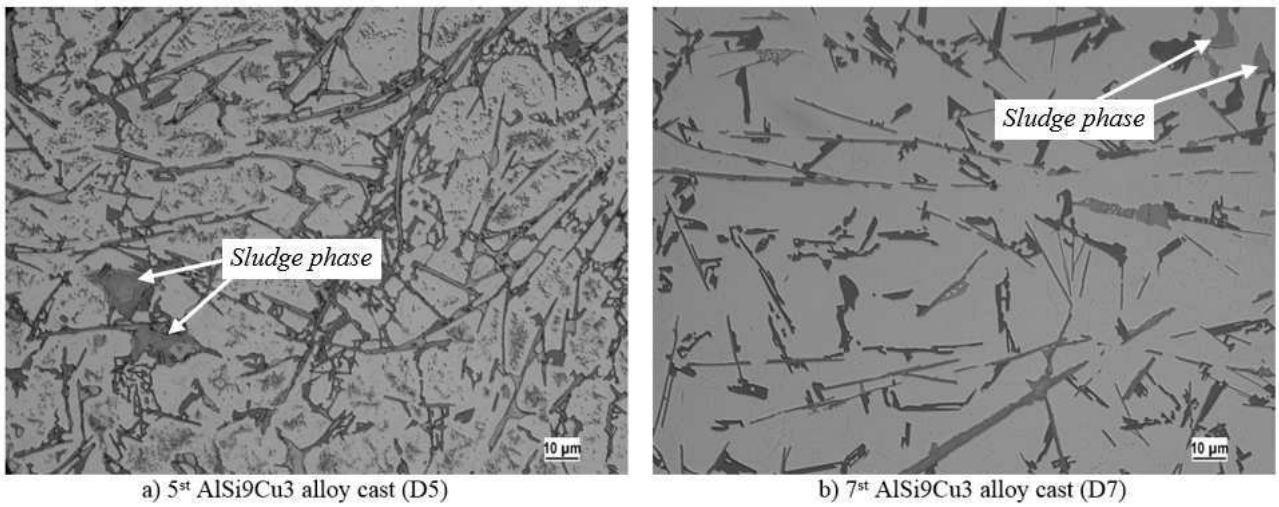

a) 5st AlSi9Cu3 alloy cast (D5) b) 7st AlSi9Cu3 alloy cast (D7)

Fig. 5 *Presence of sludge phases in microstructure*

3.2 Porosity rating

The influence of the remelting and the increasing iron content in the alloy to the porosity was evaluated based on the area porosity. From the results in tab. 6 it can be concluded that the lowest porosity was measured at the alloy D3, and in the presence of an increasing number of remelting the porosity grew only slightly. The porosity values ranged within a relatively narrow range from 0.02 to 1.23%. The highest porosity value was measured in alloy D7 after heat treatment. Fig. 6 and Fig. 7 shows an increase in porosity at alloys D7 compared to D3 alloys after natural aging and after heat treatment. In the figures shown, the porosity is represented by the red color.

Tab. 6 *Results of measurements of porosity*

Cast number		D1	D3	D5	D7
Porosity (%)	Natural aged	1.2	0.12	0.21	0.55
	Artificial aged	0.97	0.02	1.07	1.23

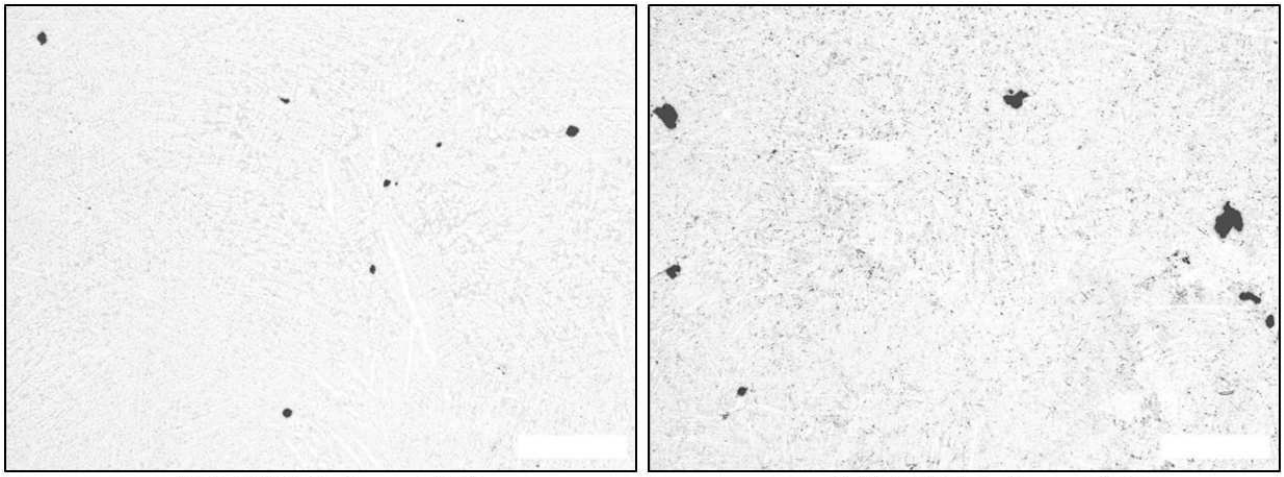

a) 3rd AlSi9Cu3 alloy cast (D3) b) 7th AlSi9Cu3 alloy cast (D7)

Fig. 6 *measurements porosity of AlSi9Cu3 alloy after Naturally aged*

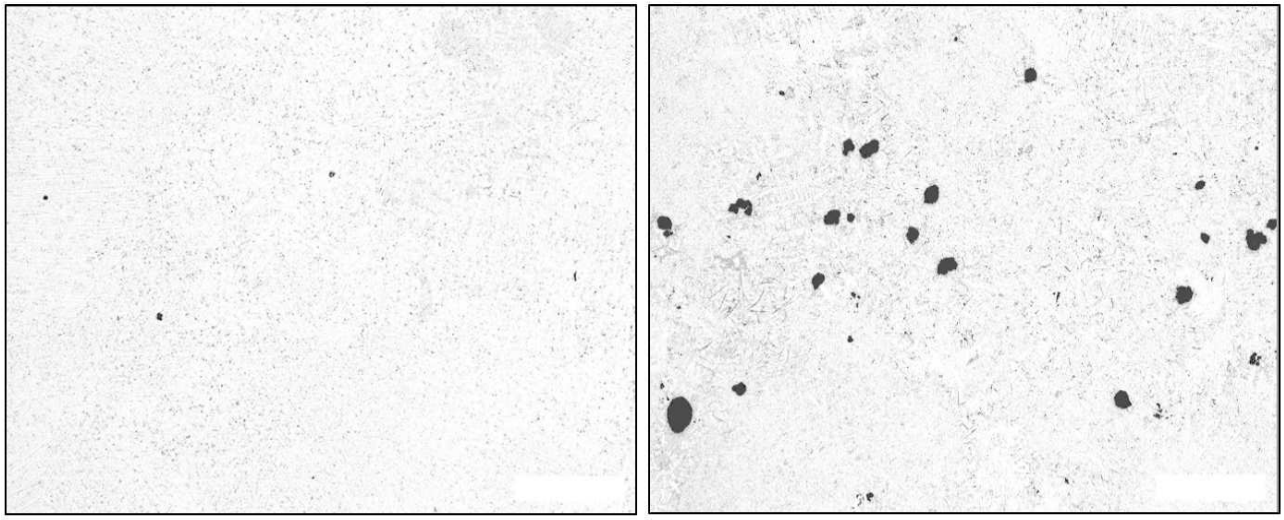

a) 3rd AlSi9Cu3 alloy cast (D3) b) 7th AlSi9Cu3 alloy cast (D7)

Fig. 7 *measurements porosity of AlSi9Cu3 alloy after Artificially aged (T5)*

4 Conclusion

The microstructural analysis of AlSi9Cu3 alloy with increased iron content documents that the expected negative effect of increasing remelting began to manifest only after the third remelting, with an occurrence of needle-like shaped iron phases. After 7th remelting a completely negative effect can be observed on microstructure (D7). The microstructure consists of an increased number of iron phases, which measured the biggest average value of their lengths and the eutectic silicon in the form of slightly coarsed grains. Microstructural analysis of the alloy after application of heat treatment showed its positive effect on the length of iron phases compared to natural aging. The reduction of iron needles and local refinement occurred especially in alloys with higher number of remelting. Eutectic silicon is the same as for alloys after natural aging observed with alloys D3 and D5 in modified morphology, while only partial spheronization is observed for alloy D7. The porosity of the investigated alloys has, in spite of

the expectations, only slightly changed. The results of measuring the distance of secondary axes of dendrites, respectively. DAS factor has not been shown to be related to the change in the number of remelting.

From the presented results it can be stated that the remelting affects negatively the resulting structure of alloys, but the application of the heat treatment has proved to be a suitable method of reducing the negative influence of remelting on the microstructure, in particular on the length of the iron phases. As the number of remelting increases, it is necessary to increase the holding temperature due to the increasing probability of the sludge formation in the melt. The results did not demonstrate sufficient correlation of remelting and change in DAS factor and porosity.

References

[1] TAYLOR, J.A. (2012). Iron-containing intermetallic phase in Al-Si based casting alloys. In: *Procedia Materials Science*. 2012. Vol 1, pp. 19-33.

[2] DINNIS, C. M. et al., (2005). As-cast morphology of iron-intermetallics in Al-Si foundry alloys, *Scripta Materialia* 53 (8), pp. 955-958.

[3] TILLOVÁ, E. – CHALUPOVÁ, M. (2009). *Štruktúrna analýza zliatin Al-Si*. EDIS Žilina. 2009. 191 s. ISBN 978-80-554-0088-4

[4] BOLIBRUCHOVÁ, D., BRŮNA, M. (2017). Impact of the Elements Affecting the Negative Iron-Based Phases Morphology in Aluminium Alloys – Summary. Results In: *Manufacturing Technology*. ISSN 1213-2489. Vol. 17, No. 5 (2017), p. 675-679.

[5] PASTIRČÁK, R. (2014). Effect of low pressure application during solidification on microstructure of AlSi alloys. In: *Manufacturing Technology*. ISSN 1213-2489. Vol. 14, No. 3 (2014), p. 397-402.

[6] BRŮNA, M., KUCHARČÍK, L. (2013). Prediction of the Porosity of Al Alloys. In: *Manufacturing Technology*. ISSN 1213-2489. Vol. 13, No. 3, pp. 296-302.

[7] PODPROCKÁ R., BOLIBRUCHOVÁ, D. (2017). The influence of manganese on elimination harmful effect of iron with different level of iron in the alloy based on Al-Si-Mg. In: *Manufacturing Technology*. ISSN 1213-2489. - Vol. 17, no. 5 (2017), pp. 815-819.

[8] CAO, X., CAMPBELL, J. (2006). *Morphology of Al_5FeSi Phase in Al-Si Cast Alloys*. Materials Transactions. 47(5), 1303-1312.

[9] FERRARO, S., BJURENSTEDT, A. & SEIFRDDINE, S. (2015). On the formation of Sludge intermetallic particles in secondary aluminium alloys. Metals & Materials Society and ASM International.

[10] KUCHARÍKOVÁ, L., TILLOVÁ, E., BELAN, J., UHRIČÍK, M. (2015). The Effect of Casting Technology on Fe Intermetallic Phases in Al-Si Cast Alloys. In: *Manufacturing Technology*. ISSN 1213-2489. Vol. 15, No. 4 (2015), p. 567-571

[11] SLÁDEK, A., PASTIRČÁK, R., BRŮNA, M., REMIŠOVÁ, A. (2017). New Application in Technological Preparations for Investment Casting Production in Aircraft Industry. In: *Manufacturing Technology*. ISSN 1213-2489. Vol. 17, No. 4 (2017), p. 842-847.

[12] MATEJKA M., BOLIBRUCHOVÁ, D. (2018). Influence of Remelting AlSi9Cu3 Alloy with Higher Iron Content on Mechanical Properties. In *Archives of Foundry Engineering*. ISSN 1897-3310. Vol. 18, No 3, pp 25-30.

10.21062/ujep/195.2018/a/1213-2489/MT/18/6/883
Copyright © 2018. Published by Manufacturing Technology. All rights reserved.